0031-3998/09/6602-0149
PEDIATRIC RESEARCH

Vol. 66, No. 2, 2009
*Printed in U.S.A.*

# Induction of *Wnt5a*-Expressing Mesenchymal Cells Adjacent to the Cloacal Plate Is an Essential Process for Its Proximodistal Elongation and Subsequent Anorectal Development

MITSUYUKI NAKATA, YUKI TAKADA, TOMORO HISHIKI, TAKESHI SAITO, KEITA TERUI, YOSHIHARU SATO, HARUHIKO KOSEKI, AND HIDEO YOSHIDA

*Department of Pediatric Surgery [M.N., T.H., T.S., K.T., Y.S., H.Y.], Chiba University Graduate School of Medicine, Chiba 260-8677, Japan; RIKEN Research Center for Allergy and Immunology [M.N., Y.T., H.K.], Yokohama 230-0045, Japan*

**ABSTRACT:** Anorectal malformations encompass a broad spectrum of congenital defects and are related to the development of the genital tubercle, including the cloacal plate and urorectal septum. To explore the cellular and molecular basis of anorectal malformations, we analyzed the pathogenetic process using two mouse models: Danforth's short tail (*Sd*) and all-*trans* retinoic acid (ATRA)-treated mice. Embryologically, the cloacal plate may be divided into distal and proximal parts, with the distal part subdivided into ventral and dorsal parts. In the two mouse models, anorectal malformations occur due to improper development of the proximal part of the cloacal plate. At 10.5 days postcoitus (dpc), in *Sd* homozygotes, there was a lack of *Shh* expression only in the cloacal plate and the endoderm around the cloacal plate. In addition, *Wnt5a* was not expressed in the mesoderm adjacent to the cloacal plate in the two mouse models, and *Axin2*, which is regulated by *Wnt* signaling, was not expressed in the dorsal part of the cloacal plate at 12.5 dpc. Based on these results, we suggest that *Wnt5a*, which is downstream of *Shh* signaling, and *Axin2* affect the development of the proximal part of the cloacal plate. **(*Pediatr Res* 66: 149–154, 2009)**

Anorectal malformations include a broad spectrum of congenital defects that frequently require acute surgical treatment in the neonatal period, because of intestinal obstruction. One of the most common anomalies is imperforate anus, a condition associated with significant chronic morbidity, especially fecal incontinence. The most severe forms of anorectal malformation are the high type, which usually involve an abnormal connection between the intestine and the genitourinary tract, and a persistent cloaca, in which distal intestinal and genitourinary tracts remain in a common channel (1). Patients with the high type or cloaca have more significant, serious long-term medical problems, for example, dysfunctional defecation and gender assignment issues. Despite its clinical relevance, the causes of anorectal malformations remain poorly understood (2,3). Accordingly, it is important to reveal the causes of anorectal malformations to potentially improve clinical management.

Received December 1, 2008; accepted March 27, 2009.

Correspondence: Mitsuyuki Nakata, M.D., Ph.D., Department of Pediatric Surgery, Chiba University Graduate School of Medicine, 1-8-1, Inohana, Chuo-ku, Chiba-shi, Chiba 260-8677, Japan; e-mail: mitchi@aurora.dti.ne.jp

Supported by special coordination fund from the Ministry of Education, Science and Sports, Japan.

The process of anal development has been shown based on anatomical and clinical observations (4–6). The molecular mechanisms underlying anal development and the pathogenesis of anorectal atresia have been studied in several model animals. Studies using knockout mice for *Shh* and *Hox* cluster genes have suggested that these gene products are essential for anorectal development. *Shh* is a secreted signaling molecule that mediates proliferation, survival, and differentiation during the development of various organs. Homozygous mutants of *Shh* exhibit massive defects in multiple organs including a persistent cloaca, complete agenesis of the vertebral column, heart-looping defects, tracheoesophageal fistula, and loss of distal limb structures (7–9). Concordantly, mutant mice lacking two zinc finger transcription factors participating in *Shh* signaling, *Gli2* or *Gli3*, exhibit imperforate anus with rectourethral fistula and anal stenosis. Furthermore, persistent cloaca is also observed in $Gli2^{+/-}Gli3^{-/-}$, $Gli2^{-/-}Gli3^{+/-}$, and $Gli2^{-/-}Gli3^{-/-}$ mice (10). Therefore, the *Shh* signaling cascade is essential for cloacal development. *HNF-3β* has been shown to regulate *Shh* expression, and its expression of *HNF-3β* in turn is regulated by *Shh* (11). *Ptc1* encodes a transmembrane[1] protein that functions as a receptor for *Shh*, and its expression is transcriptionally activated by *Shh* signaling (12,13). *Hox* cluster genes are also expressed during cloacal and anal development (14,15). Mutations in *Hoxa13* cause hand-foot–genital syndrome, an autosomal dominant disorder that profoundly affects the development of limb and genitourinary structures including the external genitalia, uterus, bladder, ureter, cervix, and rectum (16). In fetuses lacking both *Hoxa13* and *Hoxd13*, the cloacal cavity does not separate into a urogenital sinus and presumptive rectum, and subsequent development of the genital bud does not occur at all (17).

These observations suggest that the molecular circuitry operating in organogenetic processes in the kidney, lung, and intestine may also be active during anorectal development. Indeed, *Bmp4* and *Wnt5a* are expressed in the mesenchymal cells surrounding the cloacal plate, whereas *Fgf8* and *Bmp7* are expressed in the cloacal plate itself (18–22). However, the functions of these signaling molecules during cloacal development have not yet been elucidated.

**Abbreviations: ATRA,** all-*trans* retinoic acid; **BrdU,** 5-bromodeoxyuridine; **dpc,** days postcoitus; ***Sd*,** Danforth's short tail.

To address the role of these morphogenetic proteins during anorectal development, it is informative to investigate the expression of their genes during the pathogenesis of anorectal anomalies. We therefore attempted to address these issues by using two model animals of anorectal anomalies with distinct etiologies and different genetic processes, namely Danforth's short tail (*Sd*) and all-*trans* retinoic acid (ATRA)-treated mice. *Sd* is a spontaneous semidominant mutation on mouse chromosome 2 affecting the axial skeleton and the urogenital system. *Sd* heterozygotes and homozygotes display a broad range of abnormalities in the vertebral column and urogenital system. The anal opening is missing, and the embryonic cloaca persists in *Sd* homozygotes (23,24). ATRA administered to pregnant females at 9.5 days postcoitus (dpc) has been shown to induce anorectal malformations by toxic activity (25,26). Retinoic acid (RA) is essential for both normal embryonic development and correct tissue differentiation (27). The RA signal is transduced by RA receptors and retinoid-X receptors, which heterodimerize and bind to the upstream sequences of RA-responsive genes (28). However, the RA-responsive genes involved in anorectal development are mostly unknown although *Hox* cluster genes are possible candidates.

In this study, we compared the pathogenetic processes of anorectal malformation in two mouse models and further addressed the expression of these morphogenetic genes. The causes of anorectal malformation in the two mouse models are different. Therefore, any common signaling processes between these mice could help in the identification of genes responsible for anorectal malformation phenotypes.

## METHODS

***Mice.*** Wild-type ICR mice were mated overnight, and females were examined the following morning for the presence of a vaginal plug. If the plug was found in the noon, the dpc was considered 0.5. Pregnant females at 9.5 dpc were dosed by oral gavage with ATRA (100 mg/kg) suspended in sesame oil. Male and female *Sd* heterozygotes were mated and embryos in *Sd* homozygotes were obtained. Embryos at 9.5, 10.5, 12.5, and 17.5 dpc were used. All experiments were performed at least three times. All procedures were conducted according to protocols and guidelines approved by the RIKEN Yokohama Institute.

***Histologic analysis.*** Tissues were dissected out and fixed overnight at 4°C in 4% paraformaldehyde. The fixed tissues were then dehydrated, embedded in paraffin wax, and cut into 7-$\mu$m sections. Next, the sections were dewaxed, rehydrated, and stained with hematoxylin and eosin.

***Analysis of cell proliferation and cell death.*** Pregnant females were injected i.p. at 10.5 dpc with 100 mg/kg body weight of 5-bromodeoxyuridine (BrdU) (Sigma Chemical Co.) in PBS. Two hours after injection the tissue was dissected and fixed. Fixed samples were sectioned and stained as described previously (29). TUNEL analysis for detection of apoptotic cells in the cloacal plate was performed using an *in situ* apoptosis detection kit (Roche).

**In situ *hybridization for gene expression.*** Each embryo was pooled and rehydrated through a graded series of methanol. Digoxigenin-11-UTP-labeled riboprobes were prepared by *in vitro* transcription. Whole-mount *in situ* hybridization was performed as described previously with slight modifications (30). After hybridization, embryos were cleared and photographed.

## RESULTS

***Cloacal and anorectal development in wild-type,* Sd *homozygotes, and ATRA-treated mice.*** We first histologically examined cloacal and anorectal development. Sagittal sections through the cloacal or anorectal region were prepared at 9.5, 10.5, 12.5, and 17.5 dpc and stained with hematoxylin and eosin. In the wild type, anal development is anatomically subdivided into at least three distinct phases. We defined the cloacal plate as consisting of the proximal and distal parts, and the distal part was subdivided into ventral and dorsal parts (Fig. 1*L*, *M*, *N*, and *O*). In the first, the cloacal plate is formed from the surface ectoderm and the hindgut endoderm at the caudal region of the allantois base around 9.5 dpc. By 12.5 dpc, the cloacal cavity is separated into the anorectum and the urogenital sinus by the urorectal septum, and further subdivided into functionally proximal and distal regions of the cloacal plate. Finally, the anus opens at the proximal part of the cloacal plate (Fig. 1*A*, *C*, *F*, and *I*) (5).

We next examined anorectal development in the two model mice. In *Sd* homozygote compared with wild type, at 9.5 dpc, although the cloacal plate was formed, layers of ectodermal and endodermal cells were not regularly aligned (Fig. 1*B*). At 10.5 dpc, the morphologies of the cloaca were quite different between the two model mice. Extension of the cloacal plate along with the anteroposterior axis was significantly affected in *Sd* homozygotes, whereas it was morphologically intact in ATRA-treated mice (Fig. 1*D* and *E*). At 12.5 dpc, although there was outgrowth of the genital tubercles, the cloacal plate failed to extend proximodistally and, consequently, the proximal part of the cloacal plate was not formed in either case. Although the urorectal septum grew normally in these mice, their distal tips did not contact the proximal part of the cloacal plate; instead, an ectopic canal between the hindgut and urogenital sinus remained, which may contribute to the formation of a communication (fistula) between the rectum and bladder (Fig. 1*G* and *H*). At 17.5 dpc, there were very similar anorectal anomalies in the two model mice. These anomalies appeared very similar to the human high-type anorectal malformations. In the two model mice, the rectums were interrupted, the anal canals were completely missing, and an ectopic fistula between the rectum and bladder was present. The genital tubercles were also hypoplastic (Fig. 1*J* and *K*).

***ATRA-induced cell death at the dorsal part of the cloacal plate.*** In a previous study, caudal agenesis in ATRA-treated mice was found to correspond to extensive apoptotic outbursts in the tail bud mesenchyme, with a peak incidence at 24 h after ATRA treatment (31). Therefore, we examined the involvement of alterations in apoptotic outbursts and proliferation during cloacal plate extension in the two mouse models at 10.5 dpc. In the wild type, apoptotic cells were scattered throughout the ventral and dorsal parts of the cloacal plate (Fig. 2*A*). In *Sd* homozygotes, the cloacal plate was already shrunken, there were scattered TUNEL-positive cells, and the ventral and dorsal parts of the cloacal plate were not divided (Fig. 2*B*). In ATRA-treated mice, we consistently observed a noticeable increase in the number of TUNEL-positive cells in the dorsal part of the cloacal plate, while consistently observing no change in the number of TUNEL-positive cells in the ventral part of the cloacal plate (Fig. 2*C*). However, additional markers will have to be determined, which allow distinction of the ventral and dorsal part of the plate for quantitative analysis. BrdU labeling revealed that both the ectodermal and endodermal layers of the cloacal plate were mitotically active

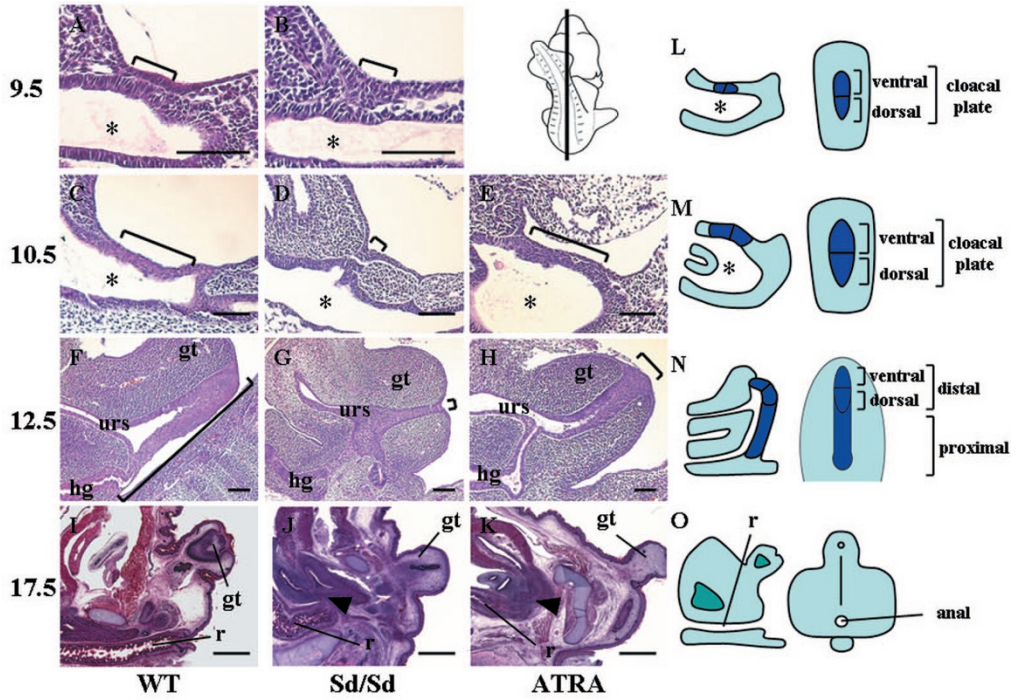


**Figure 1.** Mid-sagittal sections of the cloaca or the genital tubercle were obtained and stained with hematoxylin and eosin at 9.5 (*A*, *B*), 10.5 (*C–E*), 12.5 (*F–H*), and 17.5 dpc (*I–K*). The images are pattern diagrams from a histologic study of the midsagittal and posterior view in the wild type (*L–O*). Normal development of the cloacal plate starts and the ectoderm and endoderm are defined in the cloacal plate at 9.5 dpc (*A*, *L*). From 10.5 dpc to 12.5 dpc, the cloacal plate grows to the proximal part of the genital tubercle. The cloacal plate consists of proximal and distal parts, with the distal part divided into ventral and dorsal parts. Around the same time, the urorectal septum grows along the anteroposterior axis to the proximal part of the cloacal plate (*C*, *F*, *M*, *N*). At 12.5 dpc, the distal part of the cloacal plate and the tip of the urorectal septum fuse, and the anus opens. The hindgut differentiates into the rectum, and the urogenital sinus differentiates into the bladder (*I*, *O*). At 9.5 dpc, the cloacal plate in *Sd* homozygotes grew normally compared with the wild type (*B*), but at 10.5 dpc, it did not grow (*D*). At 12.5 dpc, the distal part was present at the tip of the genital tubercle, but the proximal part did not grow. Therefore, the urorectal septum grew normally but the anus did not open (*G*). At 17.5 dpc, in *Sd* homozygotes, the anorectal malformation was classified as a rectovesicle or rectocloacal fistula (*J*). At 10.5 dpc in ATRA-treated mice, the cloacal plate grew normally compared with the wild type (*E*), but at 12.5 dpc, it did not grow (*H*). As in *Sd* homozygotes, at 12.5 dpc, the distal part present at the tip of the genital tubercle grew but the proximal part did not. Therefore, the urorectal septum grew normally but the anus did not open. At 17.5 dpc in ATRA-treated mice, the anorectal malformation was classified as a rectovesical or rectocloacal fistula (*K*). *, cloacal cavity; gt, genital tubercle; urs, urorectal septum; hg, hindgut; r, rectum; *black bracket*, cloacal plate; *black arrow head*, fistula; scale bars, 100 $\mu$m (*A–H*) and 500 $\mu$m (*I–K*); magnification, ×200 (*A*, *B*), ×100 (*C–E*), ×50 (*F–H*), and ×20 (*I–K*).

in the wild type (Fig. 2*D*). In both mouse models, we also found a substantial number of BrdU-labeled cells in the cloacal plate (Fig. 2*E* and *F*). It is therefore likely that defects in proximodistal extension of the cloacal plate in ATRA-treated mice are due to apoptotic depletion of cloacal cells in the dorsal part. The essentially normal frequency of apoptotic cells and mitotic cells in *Sd* homozygotes suggests that the *Sd* mutation may affect cloacal development at an earlier stage.

***Expression of genes involved in genital tubercle development in two mouse models.*** Our observations prompted us to explore the signaling molecules required for the formation of the proximal part of the cloacal plate. From 10.5 to 12.5 dpc, because the morphology of the cloacal plate changes markedly, the pattern of gene expression at 10.5 dpc is particularly important. We focused on the expression of *Shh*-, *Bmp*-, *Wnt*-, and *Fgf*-related, and *Hox* cluster genes at 10.5 dpc. Moreover, we sought to identify genes whose expression was commonly affected in the two model mice. We first examined the expression of genes involved in *Shh* signal cascade signaling. The expression of *HNF-3β*, which was observed in the cloacal plate, notochord, and floor plate of the neural tube in the wild type, was reduced in *Sd* homozygotes, whereas it was unaffected in ATRA-treated mice (Fig. 3*A–C*). Furthermore, Shh was expressed in the cloacal plate, hindgut endoderm, notochord, and floor plate in the wild type (Fig. 3*D*) (8,9). In *Sd* homozygotes, the expression of *Shh* was reduced in the cloacal plate, the endoderm of the cloacal cavity, and the caudal region of the ventral neural tube but not in the hindgut endoderm (Fig. 3*E*). The expression of *Shh*, however, was unaffected in ATRA-treated mice (Fig. 3*F*). *Ptc1* was expressed at high levels in a broad domain of the mesenchyme surrounding the cloacal plate but it was not detected within the cloacal plate. The expression of *Ptc1* was unchanged in the two model mice (Fig. 3*G–I*). *Hoxa13* is expressed in the mesoderm and the endoderm of the cloaca including the cloacal plate in wild type. We observed a significant reduction in *Hoxa13* expression in *Sd* homozygotes compared with the wild type, whereas its expression was unaffected in ATRA-treated mice (Fig. 3*J–L*). Finally, we addressed the expression of *Bmp4*, *Bmp7*, *Fgf8*, and *Wnt5a* because these gene products have been shown to play essential roles during outgrowth of the genital tubercle, which is associated with the extension of the cloacal plate (21). In the wild type, *Bmp4* was expressed in the mesenchymal cells on either side of the cloacal plate

(Fig. 3*M*), and *Bmp7* was expressed in the caudal part of the cloacal plate (Fig. 3*P*). In addition, *Fgf8* was strongly expressed in the cloacal plate (Fig. 3*S*), and *Wnt5a* was expressed in the mesenchymal cells surrounding the cloacal plate (Fig. 3*V*). The expression of *Bmp4*, *Bmp7*, and *Fgf8* was substantially reduced in *Sd* homozygotes (Fig. 3*N*, *Q*, and *T*), whereas there was little change in ATRA-treated mice (Fig. 3*O*, *R*, and *U*). Strikingly, the expression of *Wnt5a* was substantially reduced in both mouse models (Fig. 3*W* and *X*).

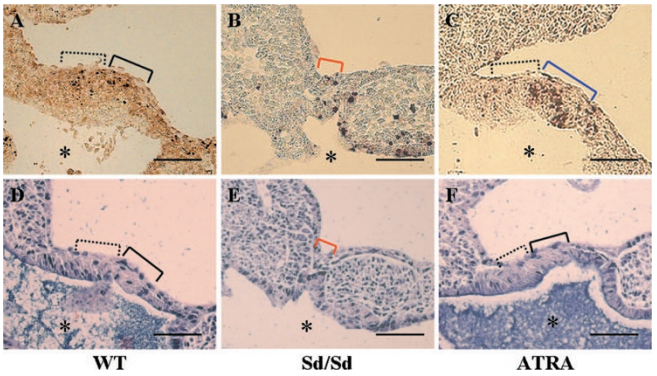


**Figure 2.** Analysis of apoptosis and cell proliferation in the cloacal plate at 10.5 dpc. In the wild type, apoptotic cells were scattered throughout the ventral and dorsal parts of the cloacal plate (*A*). In *Sd* homozygotes, the cloacal plate was already shrunken and there were scattered TUNEL-positive cells; the ventral and dorsal parts of the cloacal plate were not divided (*B*). In ATRA-treated mice, a substantial increase in TUNEL-positive cells was observed in the dorsal part of the cloacal plate, whereas there was little change in the number of TUNEL-positive cells in the ventral part (*C*). BrdU labeling revealed that both the ectodermal and endodermal layers of the cloacal plate were mitotically active in the wild type (*D*). In *Sd* homozygotes and ATRA-treated mice, there were a substantial number of BrdU-labeled cells in the cloacal plate (*E*, *F*). *, cloacal cavity; *black full bracket*, dorsal part of the cloacal plate; *black dotted bracket*, ventral part of the cloacal plate; *red bracket*, entire region of the cloacal plate in *Sd* homozygotes; *blue bracket*, positive region of the cloacal plate; and scale bars, 100 $\mu$m; magnification, $\times$100.

***The expression of* Axin2 *was reduced in the dorsal part of the cloacal plate in both* Sd *homozygotes and ATRA-treated mice.*** To gain an insight into the effect of reduced *Wnt5a* expression in both models, we examined the expression of *Axin2*, which is known to be regulated by *Wnt* and *β-catenin* signals, indicating cell proliferation (32). In the wild type at 12.5 dpc, *Axin2* was expressed at the dorsal part of the cloacal plate and bilaterally in the ectoderm of the genital tubercle (Fig. 4*A*). The expression of *Axin2* in the dorsal part of the cloacal plate was substantially reduced in both models at 12.5 dpc (Fig. 4*B* and *C*).

## DISCUSSION

Comparative analyses of *Sd* and ATRA-treated mice reveal that proximodistal elongation of the cloacal plate is a critical step for initiation of organogenesis in the anorectal region. Histologic examination indicates that defects in the cloacal plate in ATRA-treated mice appeared to occur between 10.5 and 12.5 dpc, and morphologic changes in *Sd* homozygotes were observed as soon as the cloacal plate formed at 9.5 dpc. Moreover, lack of the proximal part of the cloacal plate impaired its contact with the protruding urorectal septum and

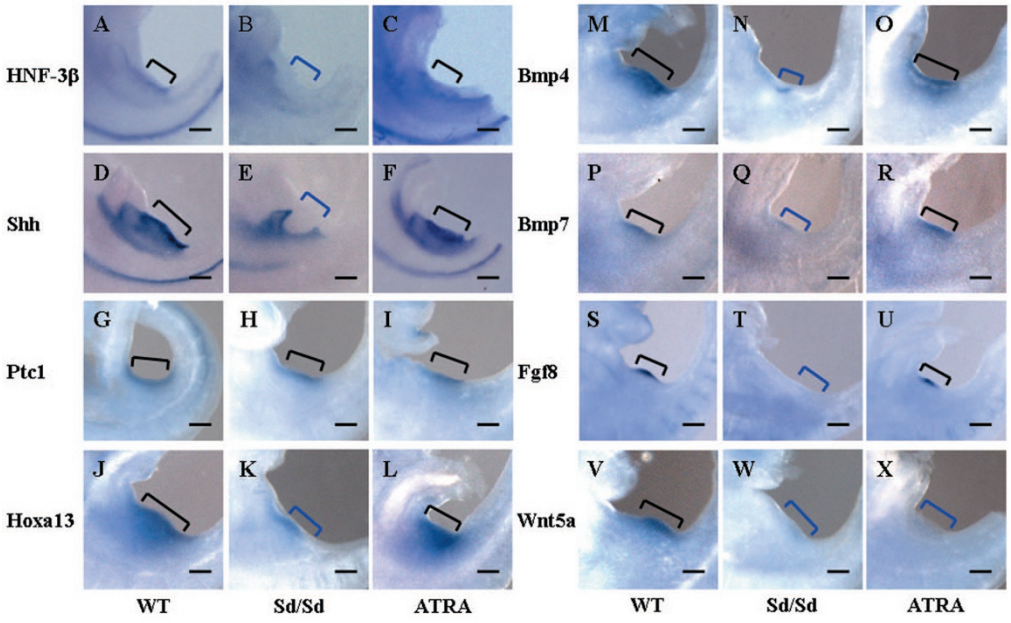


**Figure 3.** Molecular analysis of the cloaca in the mouse. Whole-mount images of lateral views to the right at 10.5 dpc (*A–X*). Black and blue brackets indicate the entire cloacal plate and the cloaca or endoderm around the cloacal plate, respectively. Black brackets indicate normal expression of genes, and blue brackets indicate weak or no expression. *HNF-3β* and *Shh* were expressed at the cloacal plate in the wild type (*A*, *D*) but not in *Sd* homozygotes (*B*, *E*). However, they were normally expressed in ATRA-treated mice (*C*, *F*). *Ptc1* was expressed adjacent to the cloacal plate in the wild type and two model mice (*G–I*). *Hoxa13* was expressed in the mesoderm and the endoderm of the cloaca including the cloacal plate in the wild type (*J*), weakly expressed in *Sd* homozygotes (*K*), and normally expressed in ATRA-treated mice (*L*). *Bmp4* was expressed in the mesoderm on either side of the cloacal plate in the wild type (*M*), very weakly expressed in *Sd* homozygotes (*N*), and normally expressed in ATRA-treated mice (*O*). *Bmp7* was expressed in the distal part of the cloacal plate in the wild type (*P*), weakly expressed in *Sd* homozygotes (*Q*), and normally expressed in ATRA-treated mice (*R*). *Fgf8* was strongly expressed in the cloacal plate in the wild type (*S*), not expressed in *Sd* homozygotes (*T*), and normally expressed in ATRA-treated mice (*U*). *Wnt5a* was expressed in wild type (*V*) but not expressed in the two mouse models (*W*, *X*). *Black bracket*, entire cloacal plate; *blue bracket*, negative region of the cloacal plate; scale bars, 100 $\mu$m; and magnification, $\times$20.

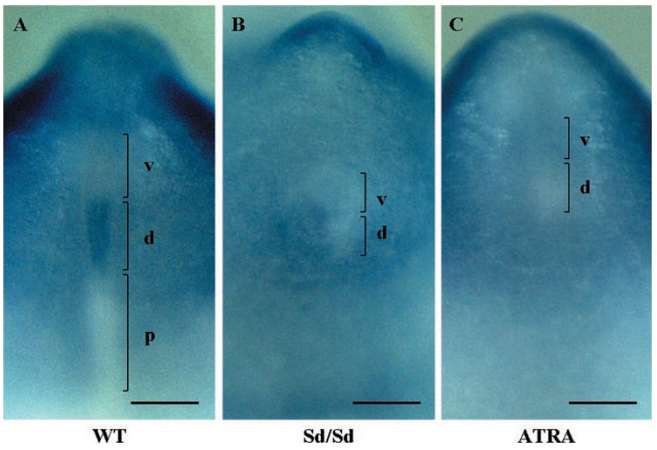


**Figure 4.** Whole-mount images of posterior views of the cloacal plate at 12.5 dpc (*A–C*). *Axin2* was expressed at the dorsal part of the cloacal plate in the wild type (*A*) but not expressed in the two mouse models (*B*, *C*). v, ventral part of the cloacal plate; d, dorsal part of the cloacal plate; p, proximal part of the cloacal plate; scale bars, 100 $\mu$m; magnification, ×40.

subsequent anal opening in the two mouse models of anorectal anomalies. Because anorectal anomalies in both models are phenocopies of high-type anorectal malformations in human patients, defects in this process may be responsible for some human forms of anal atresia, although the etiology may vary (24,25).

Our findings further suggest that induction of *Wnt5a*-expressing mesenchymal cells around the cloacal plate at 10.5 dpc is important for promoting its elongation. Because apoptotic cells predominantly accumulate in the dorsal part of the cloacal plate in ATRA-treated mice, it is likely that these cells promote elongation of the cloacal plate on the receipt of inductive signals from *Wnt5a*-expressing mesenchymal cells. The lack of *Axin2* expression in the dorsal part of the cloacal plate at 12.5 dpc in both models suggests that *Wnt5a* is functional at least in the genital tubercle. Expression of genes is important in the dorsal part of the cloacal plate at 10.5 dpc. But in the wild type at 10.5 dpc, *Axin2* in the dorsal part of the cloacal plate was expressed only weakly. The expression of *Axin2* was not defined in either *Sd* homozygotes or ATRA-treated mice at 10.5 dpc, because it was assumed that *Wnt5a* expression began at 10.0 dpc. However, the lack of *Axin2* expression in the dorsal part of the cloacal plate at 12.5 dpc suggests that the induction of *Wnt5a*-expressing mesenchymal cells adjacent to the cloacal plate may be a bottleneck in the process of proximodistal elongation of the cloacal plate. This may be the mechanism common to both the *Sd* mutation and exogenous ATRA phenotypes.

A loss-of-function mutation of *Wnt5a* affects the outgrowth of not only the axis and limb buds but also the genital tubercle (19). Conditional depletion of *β-catenin* in the genital tubercle leads to hypoplasia of the genital tubercle and its derivatives (33). Therefore, the dorsal part of the cloacal plate may be defined as the proliferating zone for elongation of the proximal part of the cloacal plate. In $Hox13^{GFP}$ mutants with hypospadius, the cloacal plate could be functionally divided into two regions during the process of urethra formation (34). Although the impact of *Wnt5a* on cloacal development has not been determined, it is possible that similar molecular circuitry operates during development of the cloacal plate and genital tubercle.

Different molecular pathways in the two models may be responsible for impaired induction of *Wnt5a*-expressing mesenchymal cells. In *Sd* homozygotes, *Shh* or *Hoxa13*, or both, may be involved. Because a lack of *Shh* affects cloacal development, a significant reduction of *Shh* expression in the cloacal plate in *Sd* homozygotes may participate. Notably, the absence of *Shh* signaling was previously reported to cause a substantial reduction of *Fgf8*, *Bmp4*, *Bmp7*, and *Wnt5a* expression in the genital tubercle (18–22). It is possible that reduced expression of *Shh* triggers the down-regulation of *Fgf8*, *Bmp4*, *Bmp7*, and *Wnt5a* expression in the cloacal plate and surrounding mesenchyme or causes the induction of cells expressing these genes. Indeed, in *Shh* null mutants, *Wnt5a* expression is substantially reduced in the genital tubercle (18). Because the expression of *Hoxa13* is also under the regulation of *Shh* in the genital tubercle and limb buds, reduction of *Hoxa13* expression in *Sd* homozygotes may also be due to reduced expression of *Shh* (35). In contrast, down-regulation of *Wnt5a* in ATRA-treated mice may not involve the *Shh* pathway because the expression of genes other than *Wnt5a* and *Axin2* are not altered. It is possible that RA directly regulates the expression of *Wnt5a*, as has been demonstrated in various tumor cell lines (36,37). This may correspond to some extent with the complex clinical spectrum of human anorectal malformations.

In summary, our results indicate that the *Sd* mutation affects the *Shh* signaling cascade, by down-regulating the expression of *Wnt5a*, which may lead to disrupted development of the proximal part of the cloacal plate. Similarly, development of the proximal part of the cloacal plate is disrupted in ATRA-treated mice, which may be due to down-regulation of *Wnt5a* expression.

***Acknowledgment.*** We thank Dr. Achim Gossler for kindly providing the *Sd* mouse.

## REFERENCES

1. Hendren WH 1998 Cloaca, the most severe degree of imperforate anus: experience with 195 cases. Ann Surg 228:331–346
2. Santulli TV, Schullinger JN, Kiesewetter WB, Bill AH Jr 1971 Imperforate anus: a survey from the members of the Surgical Section of the American Academy of Pediatrics. J Pediatr Surg 6:484–487
3. Stevenson R 1993 Human Malformations and Related Anomalies. Oxford University Press, London, pp 493–499
4. Kluth D, Hillen M, Lambrecht W 1995 The principles of normal and abnormal hindgut development. J Pediatr Surg 30:1143–1147
5. Sasaki C, Yamaguchi K, Akita K 2004 Spatiotemporal distribution of apoptosis during normal cloacal development in mice. Anat Rec A Discov Mol Cell Evol Biol 279:761–767
6. Fritsch H, Aigner F, Ludwikowski B, Reinstadler-Zankl S, Illig R, Urbas D, Schwarzer C, Longato S 2007 Epithelial and muscular regionalization of the human developing anorectum. Anat Rec (Hoboken) 290:1449–1458
7. Ming JE, Roessler E, Muenke M 1998 Human developmental disorders and the Sonic hedgehog pathway. Mol Med Today 4:343–349
8. Ingham PW, McMahon AP 2001 Hedgehog signaling in animal development: paradigms and principles. Genes Dev 15:3059–3087
9. Ramalho-Santos M, Melton DA, McMahon AP 2000 Hedgehog signals regulate multiple aspects of gastrointestinal development. Development 127:2763–2772
10. Mo R, Kim JH, Zhang J, Chiang C, Hui CC, Kim PC 2001 Anorectal malformations caused by defects in sonic hedgehog signaling. Am J Pathol 159:765–774
11. Echelard Y, Epstein DJ, St-Jacques B, Shen L, Mohler J, McMahon JA, McMahon AP 1993 Sonic hedgehog, a member of a family of putative signaling molecules, is implicated in the regulation of CNS polarity. Cell 75:1417–1430

12. Goodrich LV, Johnson RL, Milenkovic L, McMahon JA, Scott MP 1996 Conservation of the hedgehog/patched signaling pathway from flies to mice: induction of a mouse patched gene by Hedgehog. Genes Dev 10:301–312
13. Marigo V, Davey RA, Zuo Y, Cunningham JM, Tabin CJ 1996 Biochemical evidence that patched is the Hedgehog receptor. Nature 384:176–179
14. Dolle P, Izpisua-Belmonte JC, Brown JM, Tickle C, Duboule D 1991 HOX-4 genes and the morphogenesis of mammalian genitalia. Genes Dev 5:1767–1776
15. Scott V, Morgan EA, Stadler HS 2005 Genitourinary functions of Hoxa13 and Hoxd13. J Biochem 137:671–676
16. Goodman FR, Bacchelli C, Brady AF, Brueton LA, Fryns JP, Mortlock DP, Innis JW, Holmes LB, Donnenfeld AE, Feingold M, Beemer FA, Hennekam RC, Scambler PJ 2000 Novel HOXA13 mutations and the phenotypic spectrum of hand-foot-genital syndrome. Am J Hum Genet 67:197–202
17. Warot X, Fromental-Ramain C, Fraulob V, Chambon P, Dolle P 1997 Gene dosage-dependent effects of the Hoxa-13 and Hoxd-13 mutations on morphogenesis of the terminal parts of the digestive and urogenital tracts. Development 124:4781–4791
18. Perriton CL, Powles N, Chiang C, Maconochie MK, Cohn MJ 2002 Sonic hedgehog signaling from the urethral epithelium controls external genital development. Dev Biol 247:26–46
19. Yamaguchi TP, Bradley A, McMahon AP, Jones S 1999 A Wnt5a pathway underlies outgrowth of multiple structures in the vertebrate embryo. Development 126:1211–1223
20. Haraguchi R, Suzuki K, Murakami R, Sakai M, Kamikawa M, Kengaku M, Sekine K, Kawano H, Kato S, Ueno N, Yamada G 2000 Molecular analysis of external genitalia formation: the role of fibroblast growth factor (Fgf) genes during genital tubercle formation. Development 127:2471–2479
21. Haraguchi R, Mo R, Hui C, Motoyama J, Makino S, Shiroishi T, Gaffield W, Yamada G 2001 Unique functions of Sonic hedgehog signaling during external genitalia development. Development 128:4241–4250
22. Suzuki K, Bachiller D, Chen YP, Kamikawa M, Ogi H, Haraguchi R, Ogino Y, Minami Y, Mishina Y, Ahn K, Crenshaw EB 3rd, Yamada G 2003 Regulation of outgrowth and apoptosis for the terminal appendage: external genitalia development by concerted actions of BMP signaling. Development 130:6209–6220
23. Paavola LG, Wilson DB, Center EM 1980 Histochemistry of the developing notochord, perichordal sheath and vertebrae in Danforth's short-tail (Sd) and normal C57BL/6 mice. J Embryol Exp Morphol 55:227–245
24. Favre A, Briano S, Mazzola C, Brizzolara A, Torre M, Cilli M, Sanguineti M, Martucciello G 1999 Anorectal malformations associated with enteric dysganglionosis in Danforth's short tail (Sd) mice. J Pediatr Surg 34:1818–1821
25. Bitoh Y, Shimotake T, Kubota Y, Kimura O, Iwai N 2001 Impaired distribution of retinoic acid receptors in the hindgut-tailgut region of murine embryos with anorectal malformations. J Pediatr Surg 36:377–380
26. Iulianella A, Beckett B, Petkovich M, Lohnes D 1999 A molecular basis for retinoic acid-induced axial truncation. Dev Biol 205:33–48
27. Maden M 2000 The role of retinoic acid in embryonic and post-embryonic development. Proc Nutr Soc 59:65–73
28. Kastner P, Mark M, Ghyselinck N, Krezel W, Dupe V, Grondona JM, Chambon P 1997 Genetic evidence that the retinoid signal is transduced by heterodimeric RXR/RAR functional units during mouse development. Development 124:313–326
29. Bellusci S, Furuta Y, Rush MG, Henderson R, Winnier G, Hogan BL 1997 Involvement of Sonic hedgehog (Shh) in mouse embryonic lung growth and morphogenesis. Development 124:53–63
30. Wilkinson DG 1992 In Situ Hybridization: A Practical Approach. Oxford University Press, Oxford, 1992
31. Shum AS, Poon LL, Tang WW, Koide T, Chan BW, Leung YC, Shiroishi T, Copp AJ 1999 Retinoic acid induces down-regulation of Wnt-3a, apoptosis and diversion of tail bud cells to a neural fate in the mouse embryo. Mech Dev 84:17–30
32. Jho EH, Zhang T, Domon C, Joo CK, Freund JN, Costantini F 2002 Wnt/beta-catenin/Tcf signaling induces the transcription of Axin2, a negative regulator of the signaling pathway. Mol Cell Biol 22:1172–1183
33. Lin C, Yin Y, Long F, Ma L 2008 Tissue-specific requirements of beta-catenin in genitalia development. Development 135:2815–2825
34. Morgan EA, Nguyen SB, Scott V, Stadler HS 2003 Loss of Bmp7 and Fgf8 signaling in Hoxa13-mutant mice causes hypospadia. Development 130:3095–3109
35. Robertson KE, Tickle C, Darling SM 1997 Shh, Fgf4 and Hoxd gene expression in the mouse limb mutant hypodactyly. Int J Dev Biol 41:733–736
36. Blanc E, Roux GL, Benard J, Raguenez G 2005 Low expression of Wnt-5a gene is associated with high-risk neuroblastoma. Oncogene 24:1277–1283
37. Saitoh T, Katoh M 2002 Expression and regulation of WNT5A and WNT5B in human cancer: up-regulation of WNT5A by TNFalpha in MKN45 cells and up-regulation of WNT5B by beta-estradiol in MCF-7 cells. Int J Mol Med 10:345–349